

Reactions within *p*-Difluorobenzene/Methanol Heterocluster Ions: A Detailed Experimental and Theoretical Investigation

Kevin S. Shores, Jay P. Charlebois, Chi-Tung Chiang, Robert L. DeLeon, Marek Freindorf,[†] Thomas R. Furlani,[†] and James F. Garvey*

Department of Chemistry, University at Buffalo, State University of New York at Buffalo, Buffalo, New York 14260-3000

Received: September 22, 2008; Revised Manuscript Received: January 9, 2009

The reactivity of *p*-difluorobenzene/methanol cluster ions has been investigated by using triple quadrupole mass spectrometry and DFT calculations. The present study was performed in light of a recent investigation of *p*-difluorobenzene/methanol (P = F-C₆H₄-F and M = CH₃OH) heterocluster ions where the solvent-catalyzed formation of *p*-fluoroanisole (A = CH₃O-C₆H₄-F) was observed in P(M)₂⁺ clusters and *not* in PM⁺ clusters. The results of our mass selected cluster ion study and theoretical calculations confirm that a single extra molecule of methanol can lower the reaction activation energy barrier in agreement with previous work for smaller clusters (PM⁺ and P(M)₂⁺). However, we also observe that P(M)₃⁺ and P(M)₄⁺ clusters undergo evaporative loss of neutral methanol to establish the P(M)₂⁺ cluster before reacting. P(M)_{n>4}⁺ clusters are capable of reacting through multiple pathways, in some cases generating a 1,4-dimethoxybenzene (B = CH₃O-C₆H₄-OCH₃) product via two separate substitution reactions within the same cluster ion. DFT calculations were employed to model the structures of the parent cluster ions, and transition state calculations were used to evaluate the activation energy for the *p*-fluoroanisole-forming substitution reaction. The calculations suggest that the reaction proceeds through a transition state containing a six-member hydrogen-bonded ring involving a reacting methanol and a second methanol that significantly lowers the activation energy.

I. Introduction

Molecular clusters present an ideal environment for observing factors that drive a chemical reaction, without outside interferences.^{1–20} Frequently, intracluster reactions are solvent catalyzed, in that a minimum number of solvent molecules are needed for a reaction to occur. In the most extreme cases, a single solvent molecule can significantly lower the activation barrier and allows a reaction to occur that is otherwise not observed.²¹ One example that has attracted considerable interest in recent years is an ion cluster that contains a single halogenated benzene microsolvated by varying numbers of polar molecules.^{6–12} S_N2-type substitution reactions have been observed in ion clusters of *p*-difluorobenzene,¹⁰ fluorobenzene,^{10,12} and *p,m*-chlorofluorobenzene¹¹ solvated by either ammonia, water, or methanol.

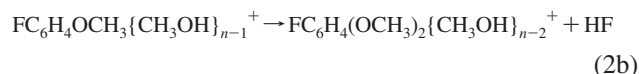
Using IR/R2PI spectroscopy coupled with high-level ab initio calculations, Brutschy et al. studied the reactivity and structure of *p*-difluorobenzene and methanol cluster ions and observed that the S_N2 substitution reaction is highly dependent on the number of solvent molecules.¹⁰



Although reaction 1 is exothermic by 100 kJ/mol, this substitution reaction is not observed in bimolecular PM⁺ clusters (where P = F-C₆H₄-F and M = CH₃OH).^{7,10} Rather, it is only observed when there are two methanols which lower the activation barrier for the substitution reaction. This effect is likely due to the special nature of the structure of the P(M)₂⁺ parent cluster.^{6,10} Ab initio geometry optimizations of P(M)_{n=1–3}⁺ clusters have shown that

small clusters contain relatively strong H-bonds between the methanols and the *p*-difluorobenzene cation.^{6,10}

In this present study, we report the results of our tandem mass spectrometric investigation of *p*-difluorobenzene/methanol cluster ions. Initially, we generate large neutral heteroclusters with the use of a Campargue-type continuous molecular beam source.^{23–25} A major advantage of the Campargue-type source is that it forms very large neutral clusters (1000+ molecules). The intense neutral cluster beam is skimmed and collimated two times before undergoing electron impact ionization. A small fraction of the neutral clusters are ionized and are then guided into a triple quadrupole mass spectrometer through a series of focusing electrostatic lenses. Energy absorbed through electron impact promotes extensive evaporative loss of neutral molecules, which lowers the overall vibrational energy of the parent cluster. This results in the formation of very cold and stable cluster ions containing up to 10 or more molecules whose reactivity may then be analyzed by tandem mass spectrometry. As already seen by Brutschy et al., our collision-induced dissociation (CID) analysis of the P(M)₂⁺ cluster reveals that the energy barrier for the substitution reaction is lowered by a single solvent molecule, as depicted by eq 1. As also previously reported, CID of PM⁺ clusters only result in evaporative loss of methanol. An interesting observation, shown in eq 2a, is made for larger *p*-difluorobenzene/methanol clusters.



where $n \geq 5$. These three observations detail the solvent catalyzed nature of one or more S_N2-type substitution reactions

* Corresponding author. E-mail: garvey@buffalo.edu.

[†] Present address: Center for Computational Research, University at Buffalo, State University of New York at Buffalo, Buffalo, New York.

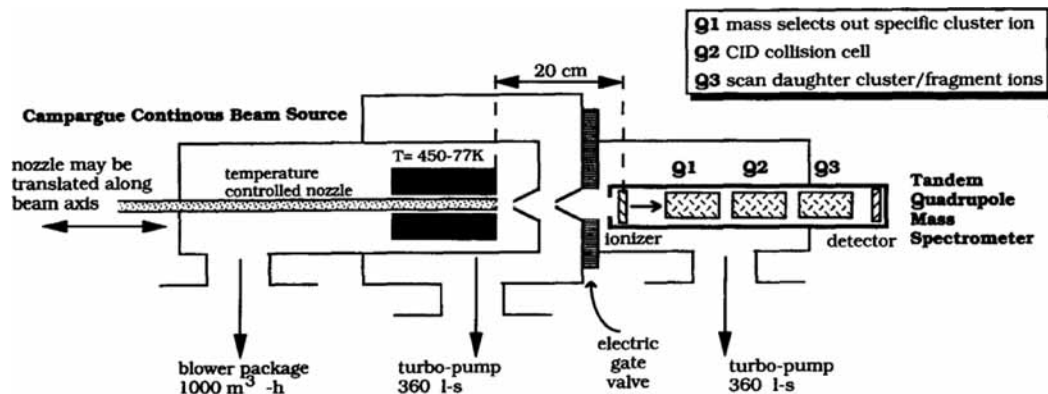


Figure 1. Schematic of the instrument used in this work.

that occur within a cluster of *p*-dimethoxybenzene and methanol.

In this paper, we present the results of our mass spectrometric investigation of methanol microsolvated *p*-difluorobenzene cluster ions. We also present the results of DFT calculations used to model the structures of the parent *p*-difluorobenzene/methanol cluster ions. To better understand the dynamics of the intracuster solvent-catalyzed substitution reactions, we have also performed transition state calculations starting with $P(M)^+$, $P(M)_2^+$, and $P(M)_5^+$ optimized geometries. The results of our studies demonstrate the dependence of chemical reactions on the structures of the parent cluster ions and reveal the means by which a single methanol molecule lowers the activation barrier for reactions.

II. Experimental Section

Instrumentation. The equipment used in this work consists of a continuous molecular beam source coupled to a triple quadrupole mass spectrometer, shown in Figure 1. The reactant mixtures were introduced by passing helium gas through a bubbler containing a 50/50 mixture of *p*-difluorobenzene to methanol by volume. Since the room temperature vapor pressure of methanol is slightly greater than *p*-difluorobenzene (110 mm vs. 72 mm) this produces a seeded mixture slightly richer in methanol. The stagnation pressure was held at 2.0 atm absolute for every experiment. Neutral clusters were generated via a supersonic expansion employing a Campargue-type molecular beam source with a 250 μm nozzle. The molecular beam is then skimmed twice by successive conical nickel skimmers, the first of which is located 7.0 mm from the nozzle. The neutral cluster beam then enters the spectrometer chamber where a small fraction of the neutral clusters are ionized by an axial-mounted electron impact ionizer. The energy of the ionizing electrons was maintained at 65.0 eV in all experiments and the emission current was held at 1.00 mA. The ionized clusters are then focused into the first quadrupole (Q1) of the triple quadrupole mass spectrometer. The mass spectrometer used in this work is the commercially available C-50 (Extrel Co.) with collinear ion optics. Conventional mass spectra were obtained by mass scanning the third quadrupole (Q3) while operating Q1 and Q2 in the RF only mode. Collision-induced dissociation (CID) spectra were obtained by first mass selecting a particular cluster ion with Q1. The second quadrupole (Q2), again operating in the RF only mode, acts as an ion guide. Q2 contains a collision cell, which, during CID experiments, is filled with argon gas at a pressure of 9.0×10^{-4} Torr. A laboratory frame collision energy of 20 eV was used for all experiments, which is determined as the difference between the cluster source potential

and the DC voltage applied to Q2. Ions exiting Q2 are then mass-analyzed by using Q3. *p*-Difluorobenzene was obtained from Aldrich chemical company and is of 98% purity. Methanol was obtained from Fisher chemical company at 99.9% purity.

Calculations. Theoretical calculations were performed by using a DFT method with the B3LYP density functional and the 6-31+G* basis set.^{25,26} This level of theory has been shown in the literature to be a precise computational approach to calculations involving hydrogen bonds.²⁷ The accuracy of our calculations has been verified by comparing results of test calculations involving the B3LYP/6-31+G* and B3LYP/6-311+G(d,p) levels of theory, which indicates that the DFT approach with the 6-31+G* basis set is an excellent compromise between computational accuracy and computational efficiency. We have calculated optimal geometries of clusters consisting of methanol molecules and the *p*-difluorobenzene cation without any constraints in the gas phase, allowing C_1 symmetry of all calculated molecular systems. The bonding energy of a particular cluster was determined as an energy difference between that of the entire cluster and that of the sum of the monomer energies (the cation and the methanol molecules). The calculations were performed for a doublet electronic state, which is the ground electronic state of the system. Reaction profiles were performed with full geometry optimization of the molecular cluster for each fixed value of a reaction coordinate, which is defined as a difference between two interatomic distances, namely the fluorine-carbon interatomic distance of the cation, and the distance between the carbon atom of the cation and the oxygen atom of methanol. The reaction coordinate was gradually changed by a step of 0.2 Å, from a value of -2.2 Å to a value of 1.8 Å. The “zero” value of the reaction coordinate was assigned to the geometry corresponding to the transition state geometry of the system. The calculations have been performed with the Q-Chem program.²⁸

III. Results and Discussion

Conventional mass spectra were collected for the expansion of the mixture of *p*-difluorobenzene and methanol by using Q3 (Figure 2) while Q1 and Q2 were operated as ion guides. Singly charged clusters with masses between 75 and 450 amu are shown in Figure 2. The largest peak in Figure 2 is that of the lone *p*-difluorobenzene (P) ion. The spectrum is also dominated by a series of protonated methanol (M) peaks, ($M_{n=3-14}H^+$) that form via proton transfer reactions in neat ionized methanol clusters.²⁹ A small occurrence of the P_2^+ dimer is also noted. Clusters containing one *p*-difluorobenzene ion and one or more methanol molecules, $P(M)_{n=0-14}^+$ are also seen in the mass spectrum; however, clusters of more than one *p*-difluorobenzene

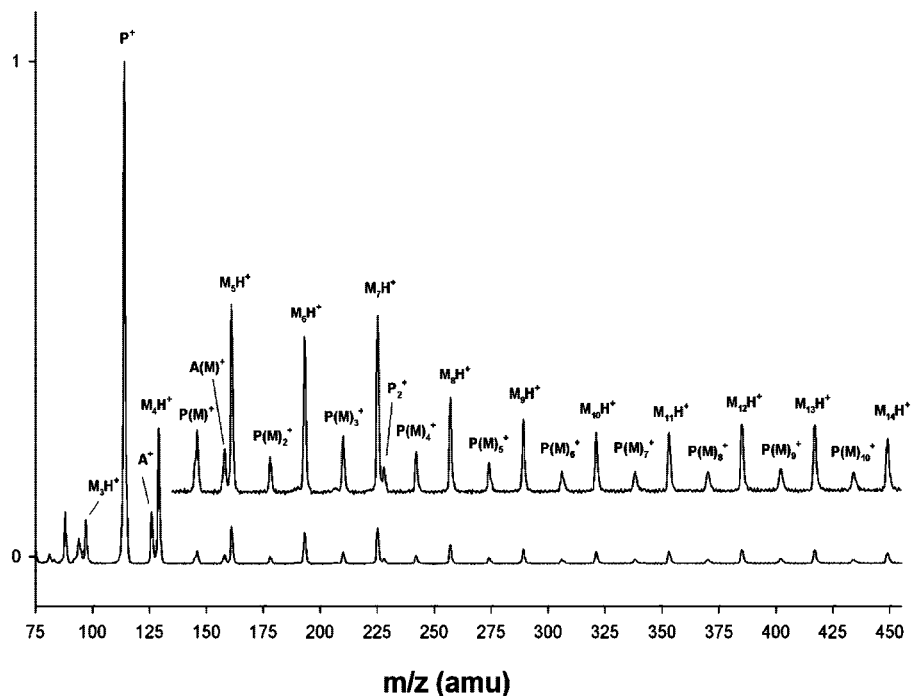


Figure 2. Survey of clusters formed in an expansion of *p*-difluorobenzene and methanol. Helium (2.0 atm) was used as a carrier gas and was diverted through a bubbler containing the reagents at 50/50 by volume, prior to the expansion. P = F-C₆H₄-F, M = CH₃OH, and A = CH₃O-C₆H₄-F. The offset portions of each portion are magnified by 5×.

along with one or more methanols are not observed in the mass spectra, likely owing to *p*-difluorobenzene's limited propensity to dimerize. *p*-Fluoroanisole clusters A(M)_{*n*=0-1}⁺, the products of intracuster substitution reactions, are also seen in the mass spectrum (where A = CH₃O-C₆H₄-F).

Sketches of the geometry optimizations of *p*-difluorobenzene/methanol cluster ions are shown in Figure 3 and include hydrogen bond distances within the cluster ions. Hydrogen bond energies of the calculated cluster ions are given in Table 1. According to Table 1, there are two stable cluster ions containing one methanol molecule and the *p*-difluorobenzene cation, namely the σ and the π cluster ions (Figure 3). In the σ cluster ion, there is a hydrogen bond between methanol's oxygen and a hydrogen of the cation and it is considered a σ -type interaction. In the π cluster ion, however, a van der Waals bond exists between methanol's oxygen and a carbon that is bonded to fluorine. This van der Waals bond has a π -type character and is based on the electrostatic attraction between the negatively charged methanol oxygen and the positively charged carbon. According to Table 1, both cluster ions have similar bonding energies of approximately 10 kcal/mol. Cluster ion structures having a hydrogen bond between the hydrogen on the methanol oxygen and a fluorine on the *p*-difluorobenzene ion were calculated but found to be relatively high in energy. Such structures undoubtedly would be important in the case of a neutral methanol and neutral *p*-difluorobenzene; however, since positively charged clusters have been studied in this work, these structures are far less important and have not been studied further. Geometry optimizations of clusters containing two methanol molecules and the *p*-difluorobenzene cation resulted in four stable conformers, namely σ - σ , σ - π , π - π , and chain (Figure 3). According to the bond energies shown in Table 1, the chain conformer is the most stable among the two-methanol cluster ions and has a van der Waals bonding energy that is almost 40% larger than the bonding energies of the other two-methanol structures.

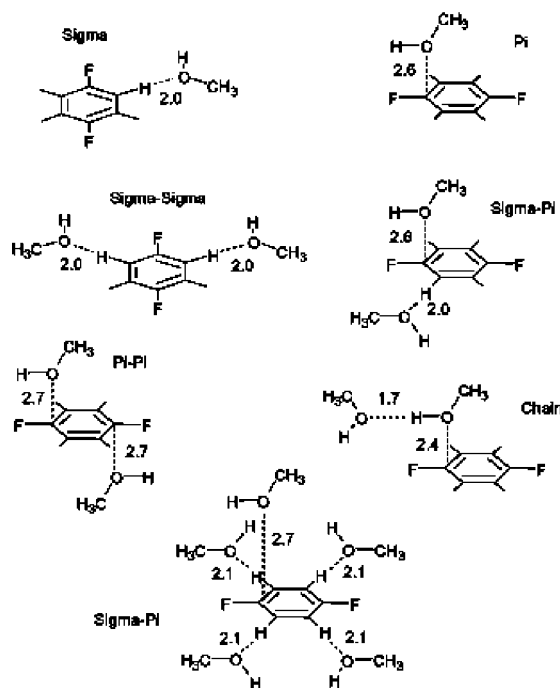


Figure 3. Sketches of the clusters containing methanol molecules and the *p*-difluorobenzene cations. For simplicity, only those aromatic hydrogen atoms are shown that are hydrogen bonded to methanol molecules. Hydrogen or van der Waals bond distances are expressed in units of angstroms.

CID spectra were obtained for the *p*-difluorobenzene/methanol P(M)_{*n*=0-9}⁺ clusters observed in the conventional mass spectrum (Figure 2). CID experiments were performed by mass selecting a parent cluster by using Q1, subjecting the parent clusters to collisions with argon gas in the collision cell located in Q2, and finally scanning the various fragmentation and reaction products by using Q3. A laboratory frame collision energy of 20 eV was used in every experiment. Under these conditions,

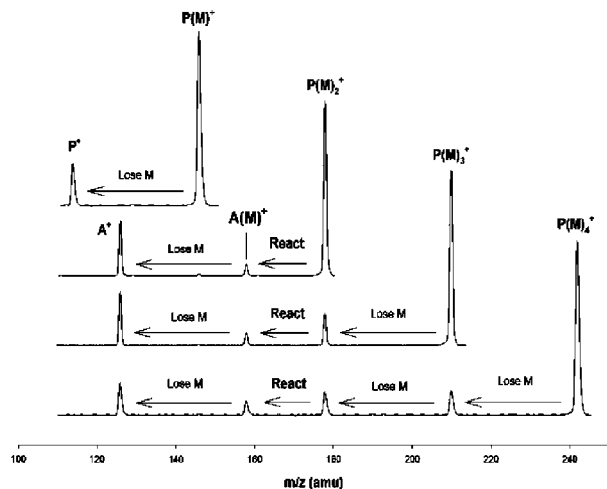


Figure 4. CID spectra of the $P(M)_{n=1-4}^+$ clusters, obtained by expanding a 50/50 mixture of *p*-difluorobenzene and methanol seeded in He(g) through a nozzle into a triple quadrupole mass spectrometer.⁸ The parent peak is the largest peak to the right in the spectrum. Individual CID spectra are superimposed and vertically offset to aid in comparison of reaction and fragmentation patterns as cluster size is increased. A = *p*-fluoroanisole, the product of a methoxy substitution on the *p*-difluorobenzene molecule.

TABLE 1: Bonding Energy of the Clusters Containing Methanol Molecules and the *p*-Difluorobenzene Cation

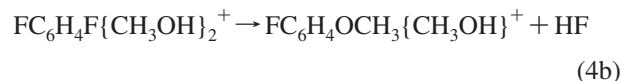
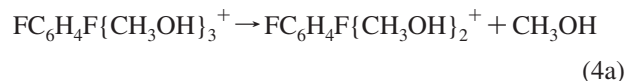
molecular cluster	bonding energy (Kcal/mol)
one-methanol structure, σ	10.6
one-methanol structure, π	11.6
two-methanol structure, $\sigma-\sigma$	20.4
two-methanol structure, $\sigma-\pi$	20.5
two-methanol structure, $\pi-\pi$	20.6
two-methanol structure, chain	26.7
five-methanol structure, $\sigma-\sigma$	44.1

it is difficult to determine the average number of collisions experienced by a given cluster; however, we roughly estimate that a cluster undergoes one or more collisions.³ The CID spectra for *p*-difluorobenzene/methanol cluster ions containing up to four methanols are shown in Figure 4. Individual spectra from each system are superimposed and offset in order to allow for an easier comparison of fragmentation and reaction channels as cluster size is increased. The size-selective nature of the methoxy substitution reaction is easily noted, as the *p*-fluoroanisole (A) product is only seen in 1:2 or larger cluster ion CID spectra. In this manner, various minor reaction and fragmentation products are visible. It is also important to note that in Figure 4, various fragmentation products are seen that result from the partial mass selection of $M_n(H_2O)H^+$ clusters. $M_n(H_2O)H^+$ clusters form readily in ionized methanol clusters and are similar in mass to the *p*-difluorobenzene/methanol clusters.^{23,30-33} To ensure that alternate isomeric products did not form in the intracluster substitution reactions other than the expected products, cluster ions of CD_3OH and CH_3OD along with *p*-difluorobenzene were also studied. CID of the 1:2 cluster ions with each solvent revealed that methoxy substitution (rather than $-CH_2OH$) occurs at the C-F carbon on *p*-difluorobenzene (data not shown).

The CID results for the PM^+ cluster are in agreement with the recent investigation of *p*-difluorobenzene/methanol clusters by Brutschy et al.^{1,5} The only process seen in PM^+ clusters is the evaporative loss of methanol (Figure 4 and eq 3).



The results for the $P(M)_2^+$ cluster are also in close agreement with previous work by Brutschy et al.^{1,5} (Figure 4). The formation of the methoxy-substituted product, *p*-fluoroanisole, is virtually the only process observed in the $P(M)_2^+$ CID spectrum (eq 1). The $P(M)_3^+$ CID spectrum is very similar to that of the $P(M)_2^+$ cluster in that a reaction occurs only after the loss of methanol and establishment of the $P(M)_2^+$ cluster (Figure 4 and eq 4a).



The $P(M)_4^+$ cluster also reacts in a similar manner in that it undergoes the evaporative loss of two neutral methanols followed by the formation of *p*-fluoroanisole and HF. We have interpreted the CID spectra for the $P(M)_3^+$ and $P(M)_4^+$ clusters (Figure 4) to indicate the evaporative loss of methanol monomers to generate the $P(M)_2^+$ cluster prior to reaction, since direct reaction products were not observed, that is, the anisole ion (A^+) solvated by two or three methanols. Given that only the $AM_{n=0,1}^+$ clusters are observed in the $P(M)_3^+$ and $P(M)_4^+$ CID spectra (no $A(M)_2^+$ and $A(M)_3^+$ clusters), it is highly unlikely that the substitution reaction occurs and is followed immediately by the evaporation of exactly one methanol from the $A(M)_2^+$ cluster and two methanols for the $A(M)_3^+$ to form the AM^+ cluster.

We have used DFT to calculate the reaction profiles between methanol molecules and the *p*-difluorobenzene cation, which are displayed in Figures 5a–c and 8. For the reaction between a single methanol molecule and the cation (Figure 5a), we have chosen the π structure of the cluster as the initial geometry of reactants (Figure 3). This choice was made due to a more suitable orientation of the reacting atoms in the π structure than in the σ structure. The transition state for the reaction of one methanol and the cation involves the aromatic carbon atom of the cation coordinated to four atoms, namely the two neighboring carbon atoms of the cation ring, and the fluorine and oxygen atoms of methanol (Figure 6). During the reaction, the hydrogen atom of methanol is transferred to the fluorine atom of the cation, and the hydrogen fluoride molecule is released as a final product. The activation energy of this reaction is larger than 30 kcal/mol, indicating that the reaction is not likely to proceed under the conditions within the mass spectrometer.

Figure 5b shows the reaction profile between two methanol molecules and the *p*-difluorobenzene cation. As an initial structure of reactants in this reaction, we have chosen the chain structure of the cluster ion, due to its stability in comparison to the other two-methanol structures. According to Figure 5b, the reaction goes through a transition state involving the aromatic carbon atom coordinated with four atoms, similar to the reaction with one methanol. However, the transition state of this reaction is strongly stabilized by the second methanol molecule due to the formation of two hydrogen bonds. One hydrogen bond exists between the hydrogen atom of methanol already bound to the cation and the oxygen atom of the other methanol. The second hydrogen bond is created during the reaction and it involves the hydrogen atom of the other methanol and the fluorine atom of the cation. The formation of the second hydrogen bond stabilizes the transition state and significantly lowers the

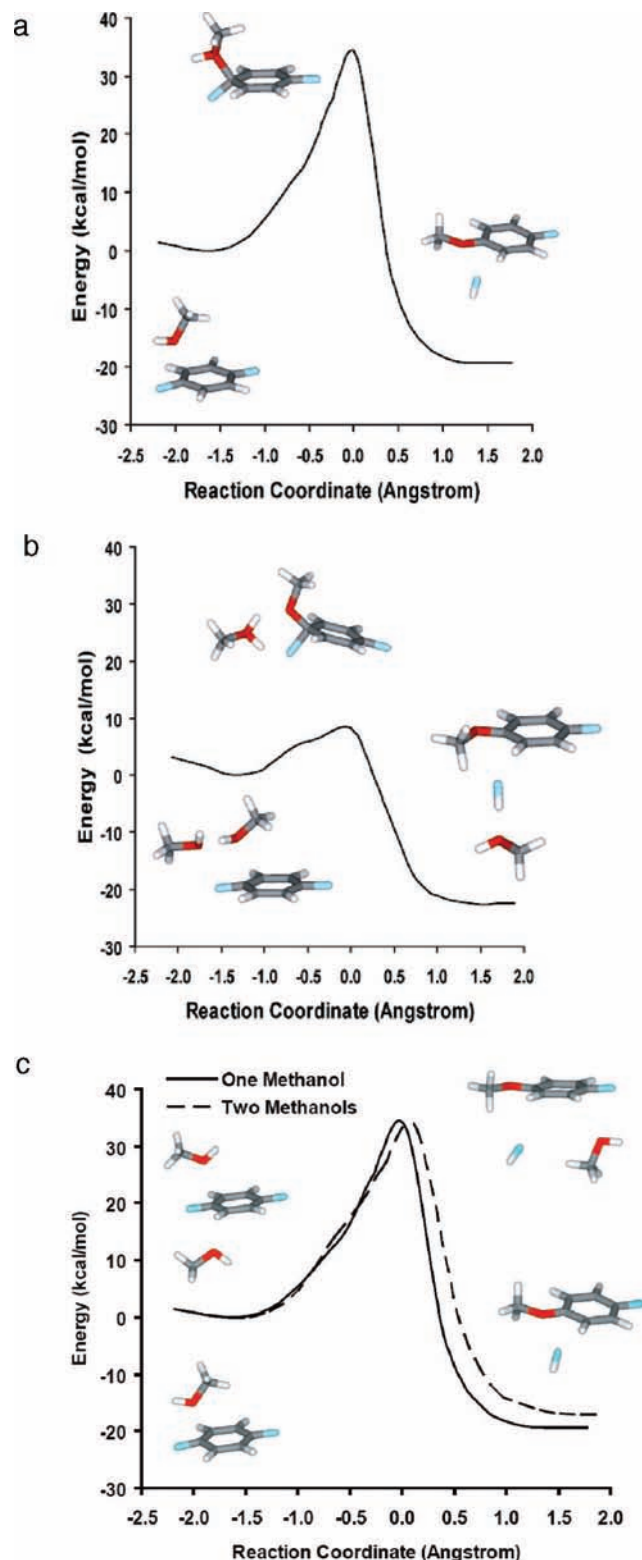


Figure 5. (a) Reaction profile between one methanol molecule and *p*-difluorobenzene cation. (b) Reaction profile between two methanol molecules and *p*-difluorobenzene cation. (c) Comparison of the reaction profile involving two methanol molecules (oriented in the opposite side of the cation aromatic ring) and *p*-difluorobenzene with the reaction profile between one methanol and *p*-difluorobenzene.

activation energy by 25 kcal/mol relative to the reaction of the cation with only one methanol molecule. In this manner, the second methanol molecule enables the reaction to occur by forming a six-member hydrogen-bonded ring, which is far more

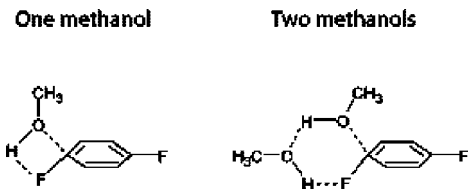


Figure 6. Sketches of the transition states occurring in the reactions involving the $P(M)^+$ and $P(M)_2^+$ clusters.

energetically stable than the four-member hydrogen-bonded ring of the transition state for the reaction with one methanol.

To determine if the proton transfer plays an important role in allowing the reaction to proceed when two methanols are present, we calculated the Mulliken charges on the important atoms in the reactants and transition states for both the one methanol and two methanol cases. (see Tables S1 and S2 in the Supporting Information). We noted that the Mulliken charges were similar for corresponding atoms in the reactants and transition states. Therefore we conclude that, while the proton transfer may play some small role in lowering the activation barrier, the stabilization of the transition state by hydrogen bonding with the second methanol is the more important contribution.

Figure 5c compares the reaction profile of the reaction involving one methanol molecule with the reaction profile of two-methanol molecules placed on the opposite side of the cation. In the case of this initial structure, the methanol molecules are not hydrogen bonded and are unable to form the transition state geometry that was calculated for the reaction starting from the chain structure (Figure 5b). As a result, the activation energy for the reaction is very similar to the reaction with only one methanol.

Clusters containing five or more methanol molecules have far more complicated CID spectra compared to those of the smaller clusters. The CID spectra for the $P(M)_{n=5-9}^+$ clusters are presented in Figure 7. $P(M)_5^+$ clusters react much differently than the $P(M)_{n=1-4}^+$ clusters. Most notably, the $P(M)_5^+$ CID spectrum contains a series of $A(M)_{n=0-4}^+$ peaks, indicating that the substitution reaction that forms *p*-fluoroanisole can occur within large heterocluster ions prior to loss of methanol. This trend is witnessed for larger clusters as well. The second unique feature of the $P(M)_5^+$ CID spectrum is the appearance of a new product ion, the 1,4-dimethoxybenzene cation ($B = \text{CH}_3\text{O}-\text{C}_6\text{H}_4-\text{OCH}_3$). This ion must result from two separate substitution reactions occurring on the same *p*-difluorobenzene cation. Spectra in Figure 4 for small clusters with $n \leq 4$ are consistent with the work of Brutschy et al.¹ and indicate a size-dependent specificity; however, the addition of a fifth methanol clearly affects the reactivity of the cluster.

Multiple geometry optimizations for clusters containing five methanol molecules and the *p*-difluorobenzene cation have also been performed. Each of the optimized structures has similar hydrogen-bonding energies of approximately 40 kcal/mol. We therefore chose to focus on the $P(M)_5^+$ structure (shown in Figure 3) with an arrangement of methanol molecules that was most similar to the geometry of the $P(M)_2^+$ chain structure (Figure 3) that was initially used to study the anisole-forming substitution reaction. Similar to the reaction in the $P(M)_2^+$ cluster, the reaction involving five methanol molecules proceeds through a transition state that is stabilized by two hydrogen bonds. The reaction profile for this reaction is shown in Figure 8. The structure of the reactant cluster has four methanol molecules bound to the cation through a σ -type hydrogen-bonding interaction, and one methanol molecule coordinated

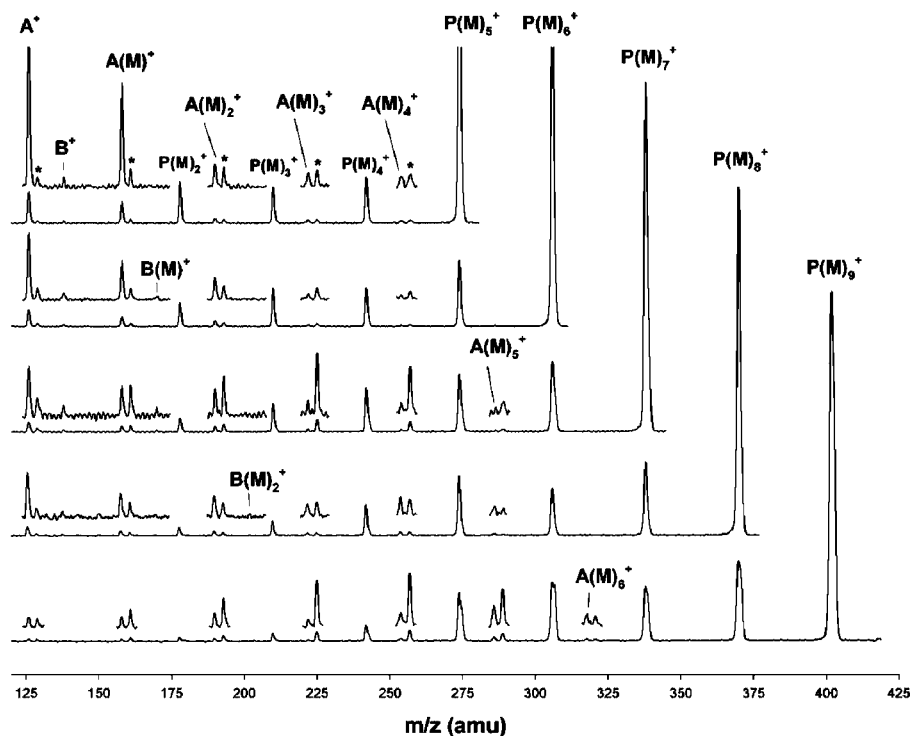


Figure 7. CID spectra of the $P(M)_n^+$ ($n = 5-9$) clusters, obtained in the same manner as in Figure 4. Individual CID spectra are superimposed and vertically offset to aid in comparison of reaction and fragmentation patterns as cluster size is increased. The offset portions of each spectrum are magnified by 5 \times . A = *p*-fluoroanisole and B = 1,4-dimethoxybenzene, the products of one and two methoxy substitutions on the *p*-difluorobenzene molecule, respectively. Peaks labeled with an asterisk (*) originate from fragmentation of $(\text{methanol})_n(\text{H}_2\text{O})\text{H}^+$ ($n = 8-12$) clusters that are partially mass selected in addition to the parent cluster.

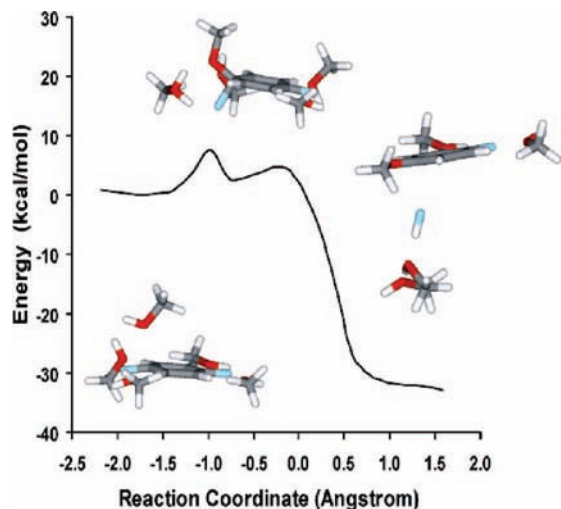


Figure 8. Reaction profile between five methanol molecules and the *p*-difluorobenzene cation. The molecular models present optimal geometries of reactants, the transition state, and the products of the reaction obtained in our calculations.

to the cation through a π -type hydrogen-bonding interaction (Figure 3). As the reaction proceeds, the second methanol is transferred from its initial position to the reaction active site. This molecular transfer requires 8 kcal/mol and is observed in our calculations as a local maximum in the reaction profile at the reaction coordinate of -1.0 \AA (Figure 8). This additional energy is required to break the hydrogen bond between the oxygen atom of the second methanol molecule and the hydrogen atom of the cation. Although we have not performed a transition state calculation for the reaction between *p*-fluoroanisole and three methanols resulting in the formation of 1,4-dimethoxybenzene (two subsequent reactions within the same cluster), our

observations strongly suggest that the reaction proceeds through a transition state involving two methanols along with the remaining C–F carbon and fluorine (six-membered hydrogen-bonded ring). With this in mind, we conclude that in order for a *p*-difluorobenzene/methanol cluster to undergo two subsequent reactions and form 1,4-dimethoxybenzene, at least four methanols must be present. In this scenario, two of the methanol molecules undergo methoxy substitution of the *p*-difluorobenzene molecule, while the additional two methanols individually lower the activation energy for each of the two reactions. The likelihood of seeing the product of both reactions significantly increases as more methanols are present in the parent cluster, since additional methanols beyond the four that are bound through π -type interactions require less energy to migrate to the transition state geometry. This trend is well pronounced in the $P(M)_{n=5-9}^+$ CID spectra (Figure 7).

IV. Conclusions

In this work, we have conducted an investigation of *p*-difluorobenzene/methanol clusters using triple quadrupole mass spectrometry and DFT calculations. The experimental results have confirmed previous observations of clusters containing up to three methanols, in that $P(M)^+$ clusters do not react, while $P(M)_2^+$ clusters react with near unity efficiency to form *p*-fluoroanisole. Larger clusters, including $P(M)_3^+$ and $P(M)_4^+$, do not react directly and must first lose one or more methanols through evaporation and form $P(M)_2^+$ before reacting to form *p*-fluoroanisole. DFT geometry optimizations and transition state calculations have demonstrated that an additional unreactive methanol molecule significantly lowers the reaction energy barrier through forming a six-membered transition state. We have also witnessed the formation of the 1,4-dimethoxybenzene cation following CID of $P(M)_5^+$ and larger clusters, which

results from two reactions within the same cluster. In this scenario, one additional methanol molecule is required to lower the activation energy for each substitution reaction. In $P(M)_5^+$ and larger clusters, four methanol molecules are bound to the *p*-difluorobenzene through σ -type interactions, while additional methanols are bound through lower strength π -type interactions and are more easily able to move within the cluster to form the transition state geometry and ultimately lower the activation barrier for the reaction.

Acknowledgment. T.R.F. gratefully acknowledges the support of NIH SBIR Grant no. 2R44GM065617-02. This work was performed in part at SUNY-Buffalo's Center for Computational Research (CCR).

Supporting Information Available: Tables S1 and S2 showing the Mulliken charges of the atoms involved in the transition state $P(M)^+$ and $P(M)_2^+$ presented in Figure 6. This material is available free of charge via the Internet at <http://pubs.acs.org>.

References and Notes

- Armentrout, P. B. *J. Anal. At. Spectrom.* **2004**, *19*, 571.
- Muntean, F.; Armentrout, P. B. *J. Chem. Phys.* **2001**, *115*, 1213.
- Armentrout, P. B. *Annu. Rev. Phys. Chem.* **2001**, *52*, 423.
- Armentrout, P. B. *J. Mass Spectrom.* **1999**, *34*, 74.
- Dedonder-Lardeux, C.; Jouvét, C.; Martrenchard-Barra, S.; Solgadi, D.; Talbot, F.; Vervloet, M.; Dimicoli, I.; Richard-Viard, M. *Chem. Phys.* **1991**, *212*, 371.
- Brutschy, B. *Chem. Rev.* **2000**, *100*, 3891.
- Brutschy, B. *Chem. Rev.* **1992**, *92*, 1567.
- Tholmann, D.; Grutzmacher, H. *J. Am. Chem. Soc.* **1991**, *113*, 3281.
- Martrenchard-Barra, S.; Dedonder-Lardeux, C.; Jouvét, C.; Rockland, U.; Solgadi, D. *J. Phys. Chem.* **1995**, *99*, 13716.
- Buchhold, K.; Reiman, B.; Djafari, S.; Barth, H.-D.; Brutschy, B.; Tarakeshwar, P.; Kim, K. S. *Chem. Phys.* **2000**, *112*, 1844.
- Riehn, C.; Buchhold, B.; Reimann, B.; Djafari, S.; Barth, H.; Brutschy, B.; Tarakeshwar, P.; Kim, K. S. *J. Chem. Phys.* **2000**, *112*, 1170.
- Djafari, S.; Barth, H.; Buchhold, B.; Brutschy, B. *J. Chem. Phys.* **1997**, *107*, 10573.
- Castleman, A. W., Jr.; Bower, K. H. *J. Phys. Chem.* **1996**, *100*, 12911.
- Dermota, T. E.; Zhong, Q.; Castleman, A. W., Jr. *Chem. Rev.* **2004**, *104*, 1861.
- Justes, D. R.; Mitric, R.; Moore, N. A.; Bonacic-Koutecky, V.; Castleman, A. W., Jr. *J. Am. Chem. Soc.* **2003**, *125*, 6289.
- Wisniewski, E. S.; Hershberger, M. A.; Castleman, A. W., Jr. *J. Chem. Phys.* **2002**, *116*, 5738.
- Folmer, D. E.; Wisniewski, E. S.; Stairs, J. R.; Castleman, A. W., Jr. *J. Phys. Chem. A* **2000**, *104*, 10545.
- MacTaylor, R. S.; Castleman, A. W., Jr. *J. Atmos. Chem.* **2000**, *36*, 23.
- Tu, Y.-P.; Holmes, J. L. *J. Am. Chem. Soc.* **2000**, *122*, 5597.
- Agorevskii, D. V.; Holmes, J. L.; Stone, J. A. *Euro. Mass Spectrom.* **1996**, *2*, 341.
- Vöhringer-Martinez; Hansmann, B.; Hernandez, H.; Francisco, J. S.; Troe, J.; Abel, B. *Science* **2007**, *315*, 497.
- Campargue, R. *J. Phys. Chem.* **1984**, *88*, 4466.
- Lytkey, M. M. Y.; DeLeon, R. L.; Shores, K. S.; Furlani, T. L.; Garvey, J. F. *J. Phys. Chem. A* **2000**, *104*, 5197.
- Rexer, E. F.; DeLeon, R. L.; Garvey, J. F. *J. Chem. Phys.* **1997**, *107*, 4760.
- Becke, A. D. *Phys. Rev. A* **1988**, *38*, 3098. (a) Lee, C.; Yang, W.; Parr, R. G. *Phys. Rev. B* **1988**, *37*, 785.
- Hehre, W. J.; Radom L.; Schleyer, P. v. R.; Pople, J. A. *Ab Initio Molecular Orbital Theory*; Wiley: New York, 1986.
- Rablen, P. R.; Lockman, J. W.; Jorgensen, W. L. *J. Phys. Chem. A* **1998**, *102*, 3782.
- Kong, J.; White, C. A.; Krylov, A. I.; Sherrill, C. D.; Adamson, R. D.; Furlani, T. R.; Lee, M. S.; Lee, A. M.; Gwaltney, S. R.; Adams, T. R.; Ochsenfeld, C.; Gilbert, A. T. B.; Kedziora, G. S.; Rassolov, V. A.; Maurice, D. R.; Nair, N.; Shao, Y.; Besley, N. A.; Maslen, P. E.; Dombroski, J. P.; Dachsel, H.; Zhang, W. M.; Korambath, P. P.; Baker, J.; Byrd, E. F. C.; Van Voorhis, T.; Oumi, M.; Hirata, S.; Hsu, C. P.; Ishikawa, N.; Florian, J.; Warshel, A.; Johnson, B. G.; Gill, P. M. W.; Head-Gordon, M.; Pople, J. A. Q-Chem 2.0. *J. Comp. Chem.* **2000**, *21*, 1532.
- Christen, W.; Even, U. *Eur. Phys. J. D* **2001**, *16*, 87–90.
- Jackson, P. *Int. J. Mass Spectrom.* **2004**, *232*, 67.
- Jiang, J. C.; Chaudhuri, C.; Lee, Y. T.; Chang, H.-C. *J. Phys. Chem. A* **2002**, *106*, 10937.
- Chaudhuri, C.; Jiang, J. C.; Wang, X.; Lee, Y. T.; Chang, H.-C. *J. Chem. Phys.* **2000**, *112*, 7279.
- Karpas, Z.; Eiceman, G. A.; Harden, C. S.; Ewing, R. G.; Smith, P. B. W. *Org. Mass Spectrom.* **1994**, *29*, 159.

JP808413C